

Article ID: 187377
DOI: 10.5586/asbp/187377

Publication History
Received: 2023-12-11
Accepted: 2024-04-17
Published: 2024-06-14

Handling Editor
Jakub Sawicki; University of Warmia and Mazury in Olsztyn, Olsztyn, Poland;
<https://orcid.org/0000-0002-1594-2418>

Authors' Contributions
JŚ, IP, JK, JS-P: Research concept and design; JŚ, JK: Collection and/or assembly of data; JŚ, IP, JK, JS-P: Data analysis and interpretation; IP, JS-P: Writing the article; IP, JK, JS-P: Critical revision of the article; JŚ, IP, JS-P: Final approval of the article

Funding
This research did not receive any external funding.

Competing Interests
No competing interests have been declared.

Copyright Notice
© The Author(s) 2024. This is an open access article distributed under the terms of the [Creative Commons Attribution License](https://creativecommons.org/licenses/by/4.0/), which permits redistribution, commercial and noncommercial, provided that the article is properly cited.

RESEARCH PAPER

Sensitivity and strength of maize roots facing different physical conditions of the growth medium

Joanna Śróbka ¹, Izabela Potocka ², Jerzy Karczewski ²,
Joanna Szymanowska-Pułka ^{2*}

¹ Industry Cooperation Office, University of Silesia in Katowice, Bankowa 12, 40-007 Katowice, Poland

² Institute of Biology, Biotechnology and Environmental Protection, University of Silesia in Katowice, Jagiellońska 28, 40-032, Katowice, Poland

* Corresponding author. Email: jsp@us.edu.pl

Abstract

The morphology of a plant's root is strongly affected by the compaction of the growth medium, the size of its particles, or the presence of non-movable obstacles. However, little is known about the effect of these characteristics on root anatomy and mechanical properties of the root tissues. Anatomical features of maize roots grown in media that varied in density and/or structure (soil, glass beads, vermiculite) were analyzed on cross-sections through the elongation and maturation zones of the roots of 14-day-old seedlings. The sections were stained for lignin and suberin to recognize the developmental stages of exodermis and endodermis. Cortex thickness, number of cortical cell layers, and diameter of the vascular cylinder (stele) were measured in both zones. The Young's modulus of the roots was determined using mechanical tensile tests. Assuming that the root can be considered a composite material, a model was used that allowed, for the first time, the estimation of the mechanical properties of the stele and cortex.

While the cell arrangement of roots grown in a medium with high density and fine movable particles (soil) was regular, roots grown in a medium with low density and light particles (vermiculite) and a medium with high density and large unmovable particles (glass beads) showed early damage of the rhizodermis and impaired cell arrangement in the cortex and vascular cylinder. In these roots, the exodermis and endodermis matured closer to the root tip than in roots from the soil. The vermiculite roots were the most outliers in terms of morphometric parameters and mechanical properties. The Young's modulus of the stele was many times greater than the Young's modulus of the cortex in the roots of all variants. Of the media used in the experiment, the soil appears to be most favorable for the maize root growth and development.

Keywords

Zea mays; root anatomy; root morphology; growth medium; exodermis; endodermis; cell arrangement; mechanical properties of plant tissue

Abbreviations

PRL - primary root length

PRD - primary root diameter

EL - elongation zone

MA - maturation zone

CT - cortex thickness

NCL - number of the cortical cell layers

DVC - diameter of the vascular cylinder

E_T , E_C , E_S - tensile Young's modulus of the root, cortex and stele, respectively

E_B - bending modulus of the root

1. Introduction

The health and general shape of the entire plant depend strongly on the environmental conditions for root develop-

ment. One of the most critical factors affecting the development and function of a root is the medium in which it grows (Kolb et al., 2017). For example, the morphological features of the root are significantly dependent on the compactness and structure of the medium. In a high compactness medium, individual roots are thicker and shorter (Konôpka et al., 2008; Loades et al., 2015), which often results in a reduction in the overall size of the root system (Grzesiak, 2009) and a change in its form (Konôpka et al., 2008; for more details, see Potocka & Szymanowska-Pułka, 2018). Roots with such morphology have increased resistance to bending and buckling (Kolb et al., 2017). A medium with a loose and porous structure and fine aggregates allows the root to grow freely. On the other hand, in a hard medium with tiny pores and large aggregates, growth is usually retarded, and roots subjected to mechanical stress under these conditions are shorter and deformed (Alexander & Miller, 1991). Using glass beads as a medium enables maintaining controlled conditions in which the growing root is exposed to mechanical stress, and the aggregate and pore sizes are uniform throughout the medium (Groleau-Renaud et al., 1998). The form of the root system strongly depends on the size of the beads; namely, when the beads, and therefore the pores between them, are relatively large, the roots are longer with short lateral roots, whereas, with smaller beads, the whole root system is shorter with a large number of lateral roots (Goss & Drew, 1972). Thus, a medium with a high density or rigid unmovable aggregates and tiny pores creates conditions of mechanical stress for the root, which must push through the tightly arranged components of the medium. In roots growing under such conditions, the above-mentioned morphological changes may be accompanied by modifications in cell arrangement and/or cell morphology. Indeed, roots grown in compacted soil, pressurized glass beads, and pressurized sand show an increased radial dimension of cortical cells (Hanbury & Atwell, 2005; Veen, 1982), a greater number of cortex layers (Iijima et al., 2007), and in some cases deformed cells of both the cortex and stele (Lipiec et al., 2012). However, the most significant anatomical change is the rearrangement of the cell pattern of the cap and the loss of a distinct boundary between the meristem and cap that occurred in the roots of *Hordeum vulgare* grown in pressurized glass beads (Wilson & Robards, 1979). Interestingly, a similar reorganization leading to the opening of the meristem, that is, the ingrowth of cells of the root proper to the cap side, was observed in maize roots subjected to local mechanical stress by growing into tight and rigid tubes (Potocka et al., 2011).

Plant tissues, like any material, have mechanical properties that can be estimated based on the morphological response of the material to external mechanical stimuli (Szymanowska-Pułka, 2013). To determine the mechanical moduli and parameters of materials, as well as the relationship between the deformation of the sample and the applied deforming force, mechanical tests are used. Plant roots also undergo such tests (for example, Hattori et al., 2003; Potocka et al., 2011; Tanimoto et al., 2000). But why do we want to know the mechanical properties of roots? Experiments show that stiff roots penetrate the soil better, receiving better access to water and nutrients (Clark et al., 2008). The stiffness of the material, including plant tissues, is greater the higher the values of mechanical moduli, such as Young's modulus, are (Goodno & Gere, 2020; Onoda et al., 2015), and that

is why the mechanical properties of roots are measured or estimated. Mechanical tests on roots have shown that the mechanical properties of their tissues depend on the culture conditions and the distance from the root tip (Hattori et al., 2003; Tanimoto et al., 2000). A study by Chimungu et al. (2015) indicates that the morphometric traits of root tissues and cells also affect their mechanical properties. It should also be taken into account that the different tissues that make up plant organs have different mechanical properties, meaning they can be considered composite materials (Gibson, 2012). In the root, this applies to the stiff vascular tissue and the thin-walled parenchyma cortical cells. Obviously, it is impossible to determine these properties in experiments using intact roots, but we can estimate them based on the morphological traits of the root (Onoda et al., 2015).

The objects of our study were maize roots. Maize is a model plant in many areas of botanical research. Moreover, it is a cereal crop of great importance in economics. Because it is relatively easy and inexpensive to grow and tolerates a wide range of climatic conditions, it is cultivated worldwide as a food source, animal feed, and raw materials for other products. For this reason, it seems essential to know the optimal growth conditions for this plant, especially the conditions of growth and development for its roots. The meristematic zone of the root in maize typically covers 2 mm of the distal-most part of the root. Above, in the region of about 2 to 10 mm, is the elongation zone, followed by the maturation zone (Alarcón et al., 2014). In cross-section through the mature maize root, a central stele (vascular cylinder) is present, with 6 to 10 large late metaxylem elements and finer early metaxylem and protoxylem elements on their outer sides. The protoxylem poles alternate with the primary phloem cells. Vascular tissues are surrounded by a single layer of pericycle cells that directly underlies a single layer of endodermis, with the Casparian strips providing a barrier to water and nutrients. The endodermis, the innermost cortex layer, is covered by 8 to 15 layers of parenchymatous cortical cells with numerous intercellular spaces. The outermost root layer is the rhizodermis. The layer of cortex cells, lying just below the rhizodermis, develops Casparian strips and transforms into the exodermis (Enstone et al., 2002). In maize, as in other grasses, both the endodermis and exodermis may occur in three stages of maturity: stage I, in which Casparian bands are present in the anticlinal walls, occupying up to 50% of the wall dimension in the endodermis and the entire anticlinal wall in exodermis (Enstone et al., 2002), stage II characterized by deposition of suberin lamellae between the cell wall and cell membrane, and finally, stage III in which U-shaped tertiary wall thickenings occur (Schreiber et al., 1999). Differentiation of endodermis and exodermis depends on plant species and growth conditions; namely, in plants growing under stress conditions, Casparian bands are present in both tissues closer to the root tip than in plants growing under optimal laboratory conditions (Karahara et al., 2004; Peterson, 1988). Unlike the endodermis, where the two processes are temporally and spatially separated, the exodermis develops suberin lamellae during or immediately after the Casparian bands are deposited (Enstone et al., 2002). In maize roots grown in vermiculite, Casparian bands in the endodermis typically mature about 10 mm from the root tip and in the exodermis 20 mm further (Perumalla & Peterson, 1986). The development of lignified and suberized cell layers enveloping the cortex makes them a barrier to

Table 1 Growth media used in the experiment.

Medium	Abbreviation	Description and physical characteristics	
Soil	SOIL	Sandy fraction 40%, loamy fraction 40%, remaining fractions 20%, low water permeability creating good water conditions, obtained from the experimental plot of the University of Silesia, Boguchwałowice, Poland; density 1.706 kg m ⁻³	
Glass beads 3 mm in diameter	B3	Heavy artificial substrate with large particles and small pores accumulating water	Minimum pore diameter 0.46 mm* ; density 1.341 kg m ⁻³
Glass beads 4 mm in diameter	B4		Minimum pore diameter 0.59 mm* ; density 1.295 kg m ⁻³
Vermiculite	VER	Light and porous medium with particles of a lamellar structure, providing good aeration conditions, density 0.104 kg m ⁻³	

* Method for measuring pore sizes according to Chalk et al. (2012).

apoplastic ion inflow and provides mechanical reinforcement to the root (Lux et al., 2004). Both tissues appear highly sensitive to various abiotic stresses, including mechanical stress (Enstone et al., 2002; Lux et al., 2004). For example, maize roots grown in slag have an increased amount of lignin in endodermal and exodermal cell walls (Degenhardt & Gimmeler, 2000), while endodermal cells of barley roots grown in pressurized glass beads show secondary features much earlier in the overall development of the root (Wilson & Robards, 1978).

The very first goal of this study was to investigate how different media affect the morphology of the maize roots. Since early results showed that the impact of the medium was significant, the next natural step of the study, and our second goal, was to see if and how the internal root structure was affected. To verify the hypothesis of a potential influence of the root growth medium on the differentiation of the exodermis and endodermis, we decided to extend our study with histochemical analyses that might enable us to recognize the developmental stages of these tissues. The third goal of the study was to determine the mechanical moduli of the roots growing in various media. Moreover, based on the mathematical description of the mechanical properties of composite materials (Goodno & Gere, 2020) and the mechanical model proposed by Onoda and coworkers (2015), we also made an attempt to show that anatomical traits are related to mechanical modules and that the two determine tensile stiffness and bending stiffness of the root.

2. Material and methods

2.1. Growth conditions

Maize (*Zea mays* L. subsp. *mays*, *saccharate* group, cv. *Złota Karłowa*) seeds were surface sterilized with 70% ethanol for 30 s, then with 10% commercial bleach solution for 2–4 min and washed five to six times with distilled water. Next, the seeds were imbibed with distilled water for 24 h at room temperature and germinated in Petri dishes lined with moist filter paper. After 24 h, the undamaged seeds with visible mesocotyl/coleoptile were transferred into cylindrical containers (30 cm in height and 15 cm in diameter) filled with one of four types of media: (1) sandy loam soil (coming from the experimental plot and sieved before filling the containers)

– SOIL, (2) glass beads 3 mm in diameter – B3, (3) glass beads 4 mm in diameter – B4, (4) vermiculite – VER (detailed description in Table 1). The media varied in density measured as a mass-to-volume ratio and in particle sizes.

The soil is a natural substrate whose small particles (compared to the root diameter) can be pulled apart by the growing root. It is of high density and is easily permeable to water, providing good irrigation conditions. Glass beads are a high-density substrate with heavy, unmovable particles and tight pores (Goss & Drew, 1972) that may accumulate water. Vermiculite is a light, well-aerated medium with a density seven-tenths times less than soil density (Table 1) and with movable particles. It is a clay material characterized by a layered crystalline structure.

The sizes of the glass beads used in the experiment were chosen so that the pores between them were smaller than the average diameter of the root (Goss & Drew, 1972), which in maize is about 0.8–1.0 mm, depending on the root zone (Alarcón et al., 2014). The two sizes of beads were used to see if pore size could affect the root's cell pattern and mechanical properties. Both types of glass beads had a similar physical density, slightly less than the soil density.

All the seedlings were cultured for 14 days in the following conditions: 15 h of light, 9 h of dark, temperature 22 °C, relative humidity 70–80%. For the first 24 hours, the containers were covered with aluminum foil to maintain growth-promoting darkness and humidity. During the first watering, a solution of 1/2 MS was used; in each subsequent watering, tap water was applied. Excess water drained freely due to the drainage.

2.2. Macroscopic morphometry

After 14 days of culture, the seedlings were removed from the medium, and the roots were rinsed gently under tap water. Next, the above-ground part of the plant was cut off, and the roots were transferred to a laboratory tray with water in a shadowless scanner (EPSON PERFECTION V700 PHOTO). The roots were scanned with the WinRhizo software (WinRhizo Basic 2017, Regent Instruments Inc.), and the resulting images were processed with Adobe Photoshop software to remove noise and contamination from the substrate. Image analysis was performed using SmartRoot software (Guillaume

Lobet, Loic Pages, Xavier Draye, 2011). It included measurements ($n = 10$ for each variant of the experiment) of primary root length (PRL), primary root diameter (PRD), and other morphometric features of the root system that were not used in this study.

2.3. Staining and microscopy

For microscopic observations, 5–10 mm portions of the primary roots were cut, covering about 10 mm and 40 mm from the tip of the root, which corresponded to the upper border of the elongation zone (EL) and the maturation zone (MA), respectively (Alarcón et al., 2014). The fresh root fragments were embedded in a 6% low melting point agarose (Low Melting Agarose PPC, Duchefa Biochemie). The agarose block was cut with a vibrating blade microtome (Leica VT 1200) into 40–70 μm thick transverse sections. Five to six roots from each variant (SOIL, B3, B4, VER) were examined, and 20–30 sections from each zone (EL and MA) were obtained. Five to ten unstained sections of both zones and each variant were viewed under a Nikon Eclipse Ni-U microscope using an ultraviolet filter set UV-2A (excitation filter 330–380, dichroic mirror 400, barrier filter 420) and documented using a Nikon Digital Sight DS-Fi1c digital camera. The other sections were stained with either 0.1% (w/v) Sudan red 7B for 45–60 minutes to identify suberin or with 2% (w/v) phloroglucinol in ethanol/HCl for 3–5 minutes to identify lignin, five to ten sections per each staining method. Eventually, the stained sections were examined under a Nikon Eclipse 80i bright field microscope and documented using a Nikon DS-Fi2 digital camera.

2.4. Microscopic morphometry

From the cross-sections of the roots, the cortex thickness, the number of layers of the cortex cells, and the diameter of the vascular cylinder were measured. The cortex thickness (CT) and the number of the cortical cell layers (NCL), including its innermost and outermost layers, endodermis and exodermis, respectively, were determined where the cortex was not damaged and the root outline was preserved. To make measurements comparable between the variants of the experiment, CT was always measured opposite the protoxylem and early metaxylem vessels. NCL was determined according to the method presented by Vanhees et al. (2020). A layer of cells was considered a sequence of laterally adjacent cells forming a continuous array. For sections with perturbed radial cell arrangement, at least two measurements were made in the same section to obtain reliable results. In such a case, the final result was the average of the two measurements. The diameter of the vascular cylinder (DVC) was measured as the distance between the outer tangential cell walls of the pericycle on either side of the vascular cylinder. The measurement site was chosen so that the diameter intersected at least one strand of protoxylem and early metaxylem vessels and divided the vascular cylinder into two approximately equal parts. CT and DVC were measured using ImageJ (<https://imagej.nih.gov/ij/>). Six to ten measurements of the above-mentioned morphometric traits were made in both zones (EL and MA) of roots from all experiment variants (SOIL, B3, B4, VER).

2.5. Mechanical testing of the roots

Apical root segments of approximately 60 to 70 mm were collected from roots grown in the above-described experimental conditions. Only undamaged roots were selected for testing. The tests were performed using the MTS Synergie 100 testing machine (MTS System Corporation). The segments were clamped between the grips of the testing machine so that the upper and lower portions of the sample, with a length of about 10 mm, were in grips. Next, the samples were photographed, and their lengths (l , distance between the grips) and diameters (d) were measured using MATLAB software (MathWorks). Eventually, the samples were tested under tensile loading with an axial extension rate of 10 mm/min. Load and extension were measured using a load sensor with an accuracy of ± 0.001 N and an extension recorder with an accuracy of ± 10 μm , respectively, and recorded using TestWorks 4.0 software (MTS System Corporation). The Young's modulus E_T (a material's ability to resist deformation under tension) was obtained from the initial gradient of the stress-strain plot during testing within the elastic region (Loades et al., 2015). Considering the way the sample was placed in the grips of the testing machine, the tests were performed in the maturation zone of the root (above 10 mm from the root tip). The number of the tested segments of each variant were as follows: $n_{\text{SOIL}} = 11$, $n_{\text{B3}} = 10$, $n_{\text{B4}} = 9$, $n_{\text{VER}} = 11$.

2.6. Statistical analyses

2.6.1. Macroscopic morphometry

As both PRL and PRD were continuous variables, and their distribution, tested separately for each variant of the experiment, was found to be normal (based on the Shapiro–Wilk test, significance level $p = 0.05$), the parametric Analysis of Variance tests were used to detect possible differences in the mean values of these variables between variants. The ANOVA test was preceded by the Levene test of homogeneity of variance, which showed no significant differences in variances between the variants of the experiment for both PRL and PRD. Since the ANOVA test detected significant differences between the means for PRL and PRD, the *post hoc* Least Significant Differences (LSD) test was used to compare the means in pairs.

2.6.2. Microscopic morphometry

The data structure concerning CT, NCL, and DVC indicated asymmetric distribution that appeared far from normal (based on the Shapiro–Wilk test, significance level $p = 0.05$). That is why the non-parametric Kruskal–Wallis Analysis of Variance test was used to detect possible differences between the medians of the parameters from the four variants. The non-parametric Tuckey *post hoc* test of multiple comparisons was used when the Analysis of Variance detected the presence of significant differences between the variants. Differences between the traits in the two zones (EL and MA) were tested separately using the non-parametric Mann–Whitney U statistics for each experiment variant.

Table 2 Means ± standard errors of the primary root length (PRL) and the primary root diameter (PRD) of roots grown in sandy loam soil (SOIL), glass beads 3 mm in diameter (B3), glass beads 4 mm in diameter (B4) and vermiculite (VER).

	SOIL	B3	B4	VER
PRL [cm]	19.13 ± 1.26	14.19 ± 1.50	16.16 ± 1.63	22.79 ± 1.82
PRD [mm]	0.855 ± 0.032	0.839 ± 0.025	0.812 ± 0.034	0.660 ± 0.031

2.6.3. Mechanical properties

As E_T of the root segments from the four experimental variants demonstrated distribution far from normal (based on the Shapiro–Wilk test, significance level $p = 0.05$), the non-parametric Kruskal–Wallis Analysis of Variance test, followed by the Tuckey *post hoc* test of multiple comparisons were used to detect significant differences between medians.

All statistical analyses were performed using STATISTICA 13 (TIBCO Software Inc. 2017).

2.7. Estimation of mechanical properties of vascular cylinder and cortex

Two dominant root tissues that differ in mechanical properties are the cortex, composed of thin-walled cells, and the stele with rigid vascular tissues. From a mechanical point of view, the root can be regarded as a beam-shaped composite material with a circular cross-sectional area. For composite objects of such geometry, the relationship between total tensile stiffness ($E_T \cdot A$) and its components derived from material fractions is expressed by the equation (Goodno & Gere, 2020; Onoda et al., 2015):

$$E_T \cdot A = E_S \cdot A_S + E_C \cdot A_C, \quad (1)$$

where E_S and E_C represent the Young's modulus of the stele and cortex, respectively, while A is cross-section area of the composite beam ($A = \pi \cdot \left(\frac{D}{2}\right)^2$, D is a root diameter), A_S and A_C are the cross-section area of the stele and cortex, respectively, so that $A = A_S + A_C$.

The relationship between total bending stiffness ($E_B \cdot I$) and its components is similarly expressed (Onoda et al., 2015):

$$E_B \cdot I = E_S \cdot I_S + E_C \cdot I_C, \quad (2)$$

where E_B is a bending module (material's ability to resist deformation in bending), I is the second-moment area of the composite beam ($I = \frac{\pi}{64} \cdot D^4$) and I_S and I_C are the second moment of area of the stele and cortex, respectively, and $I = I_S + I_C$.

Next, E_B/E_T is calculated by dividing Equation (2) by Equation (1):

$$\frac{E_B}{E_T} = \frac{1 - \alpha^2 \cdot (1 - \beta)}{1 - \alpha \cdot (1 - \beta)}, \quad (3)$$

where $\alpha = A_S/A$ and $\beta = E_S/E_C$.

In this study, the fraction α of the stele area to the root cross-sectional area was calculated using microscopic measurements of CT (cortex thickness) and DVC (diameter of the vascular cylinder), namely $A_S = \pi(DVC/2)^2$, $A = \pi(DVC/2 + CT)^2$.

As large E_T affects higher tensile stiffness of the root, it was assumed that the ratio E_B/E_T is minimal (E_T much larger than E_B) with α obtained from the experiment. This assumption allowed the calculation of β , and then E_B , using the E_T value obtained from the tensile test. Eventually, E_S and E_C were calculated from Equations (1) and (2). Since E_B , E_S , and E_C were not derived from measurement but were estimated from a mathematical model, they were not subjected to statistical analysis.

3. Results

3.1. Quantitative analyses of the macroscopic features

Table 2 shows the average values of the primary root length (PRL) and the primary root diameter (PRD) of roots from the four experiment variants. The smallest average PRL (14.19 cm) was found in roots growing in glass beads with a diameter of 3 mm, and the largest (22.79 cm) in roots coming from vermiculite. In this characteristic, the B3 variant differed significantly from the SOIL and the VER variants and the VER variant from the B3 and B4 variants (Figure 1). Roots growing in soil were largest in diameter (0.885 mm), and roots growing in beads of both sizes were slightly thinner. Still, the differences between these variants were not statistically significant. In contrast, the roots growing in vermiculite were significantly thinner than the roots of the other variants (Figure 1).

3.2. Anatomy: arrangement of the outermost cell layers and development of the exodermis

In the elongation zone of roots growing in the soil (Figure 2A, E), the rhizodermis was well preserved, lacking damage, and adjacent cells maintained contact. In roots growing in glass beads (both 3 and 4 mm in diameter, Figure 2B, F and C, G, respectively) and in vermiculite (Figure 2D, H), some rhizodermal cells were malformed and/or damaged, and their radial dimension was reduced. In roots from the variant SOIL, neither lignin nor suberin was observed in the exodermal cell walls (Figure 2A, E). In roots grown in the other media, suberin lamellae were deposited in exodermal cells (Figure 2F–H), indicating that the exodermis had entered the second phase of development. Lignin was present in both the periclinal and anticlinal walls of most exodermal cells of roots grown in the VER variant (Figure 2D). In roots from the B4 variant, lignin was detectable exclusively in the periclinal wall of some exodermal cells (Figure 2C). Some damaged rhizodermal cells of roots from the variant VER also showed the presence of lignin (Figure 2D).

In the maturation zone, rhizodermal cells of roots of all variants were deformed (Figure 2I–P). Compared to the elon-

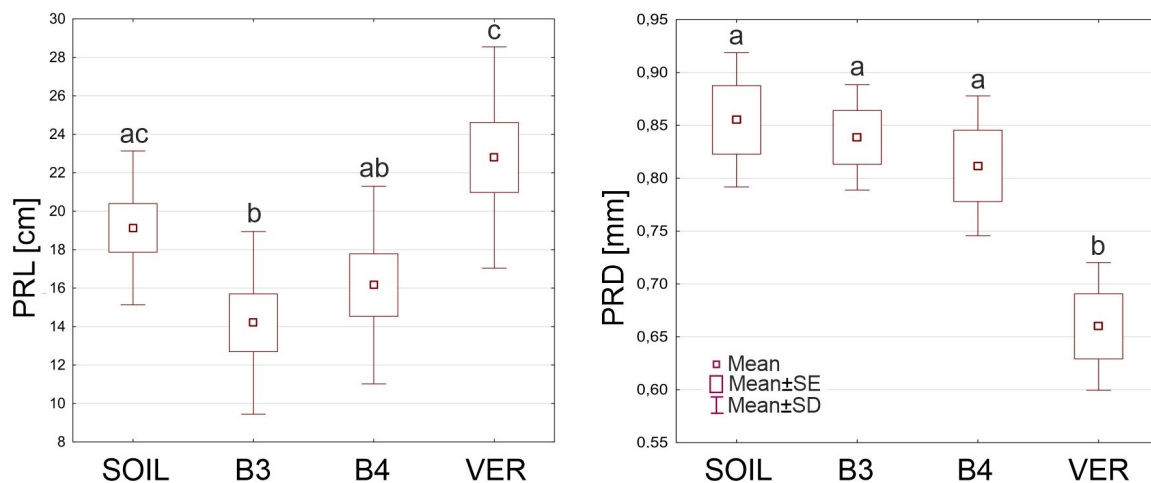


Figure 1 The primary root length (PRL) and the primary root diameter (PRD) of *Zea* roots grown in sandy loam soil (SOIL), glass beads 3 mm in diameter (B3), glass beads 4 mm in diameter (B4) and vermiculite (VER). Box and whiskers plots represent mean values (small squares), mean \pm standard error (box), and mean \pm standard deviation (whiskers). The same small letters (a, b, c) above the plots indicate statistically insignificant differences between the medians (comparison between variants using ANOVA and *post hoc* NIR test, $p < 0.05$).

gation zone, the most remarkable changes occurred in roots grown in soil whose outermost cells had lost their regular shapes, so it was difficult to distinguish the continuous rhizodermal cell layer (Figure 2I, M). Some rhizodermal cells of roots grown in vermiculite and beads were crushed or damaged (Figure 2L, N–P). On the surface of roots of the B3 variant (Figure 2J) and, less frequently, of the B4 variant (not shown), local flattening occurred due to contact with a rigid medium. In the SOIL roots, as in the EL zone, there was no detectable lignin or suberin in the walls of the outer cell layers (Figure 2I, M, respectively). Roots grown in the other media showed the presence of lignin both in the anticlinal and outer periclinal cell walls of the exodermis (Figure 2J–L) and in the VER variant, also in the vicinity of damaged rhizodermal cells (Figure 2L). Suberin lamella was detected in the exodermis of roots grown in beads of both sizes and vermiculite (Figure 2N–P). In no variant or zone were tertiary walls observed in the exodermis.

3.3. Anatomy: arrangement of the cortex cells

The cortical cells had a regular radial arrangement in cross-sections through the elongation zone of roots growing in soil. Cell sizes decreased in the direction toward the vascular cylinder. Small intercellular spaces were found mainly in the inner layers of the cortex (Figure 3A). In roots grown in beads (B3–4), the radial arrangement of cortical cells was slightly disturbed (Figure 3B–C) whereas, in roots grown in vermiculite, it was wholly lost (Figure 3D). The VER variant roots showed firmly packed deformed cells with tiny intercellular spaces (Figure 3D). In variants B3 and B4, the cells were less tightly arranged with intercellular spaces of different sizes (Figure 3B–C). The cortex cells in roots grown in beads and vermiculite were smaller in this view than in the SOIL variant.

The radial arrangement of cortical cells in the SOIL roots was preserved in the MA zone. The cells of the outer cortex layers were large, and the cells near the vascular cylinder were smaller. Intercellular spaces were slightly larger than in

the elongation zone (Figure 3E). In other variants, the radial arrangement of the cortex cells was more or less disturbed (Figure 3F–H). In B3 and B4 variants, the cells and the intercellular spaces varied in size in different cortical layers (Figure 3F, G). In the VER variant, the cells had more regular shapes (Figure 3H) than in the elongation zone (compared to Figure 3D), but they were generally smaller (Figure 3E). In roots from variant B4, many cells were deformed and, in places, collapsed or torn, as evidenced by local empty areas in the cortex (Figure 3G).

3.4. Anatomy: endodermis differentiation and cellular arrangement of the vascular cylinder

In the cross-section through both zones (EL and MA) of the roots grown in all media, the vascular cylinder was generally circular; only in some roots growing in the soil, it happened to be slightly oval (for example, Figure 4I). In roots from all variants of the experiment, in both zones, the Casparian bands were present in the endodermal cells (Figure 4A–D, M–P, respectively). In the EL zone, in roots from variants B4 and VER (Figure 4G–H), the suberin lamella had not developed yet, although it had developed in some cells of roots grown in soil (Figure 4E, Sudan red 7B staining) and in all endodermal cells of roots grown in glass beads of 3 mm diameter (Figure 4F). Moreover, in variant B3, the tangential inner walls of the endodermal cells were thickened, and the U-shaped arrangement was formed (Figure 4J). In the MA zone, suberin lamellae were present in all the endodermal cells of the roots from the B3, B4, and VER variants (Figure 4S–U), while in the roots grown in the soil, the suberin lamella was only visible in some cells (Figure 4R). In variant B3, the U-shaped endodermal walls were recognizable (Figure 4W). Thickened tangential inner walls of the endodermal cells were also present in roots from variant B4 (Figure 4O).

In all variants and both zones, the walls of early metaxylem and protoxylem elements were lignified (Figure 4C–D, M–P). The central vascular cylinder contained 4 to 5 vessels of the

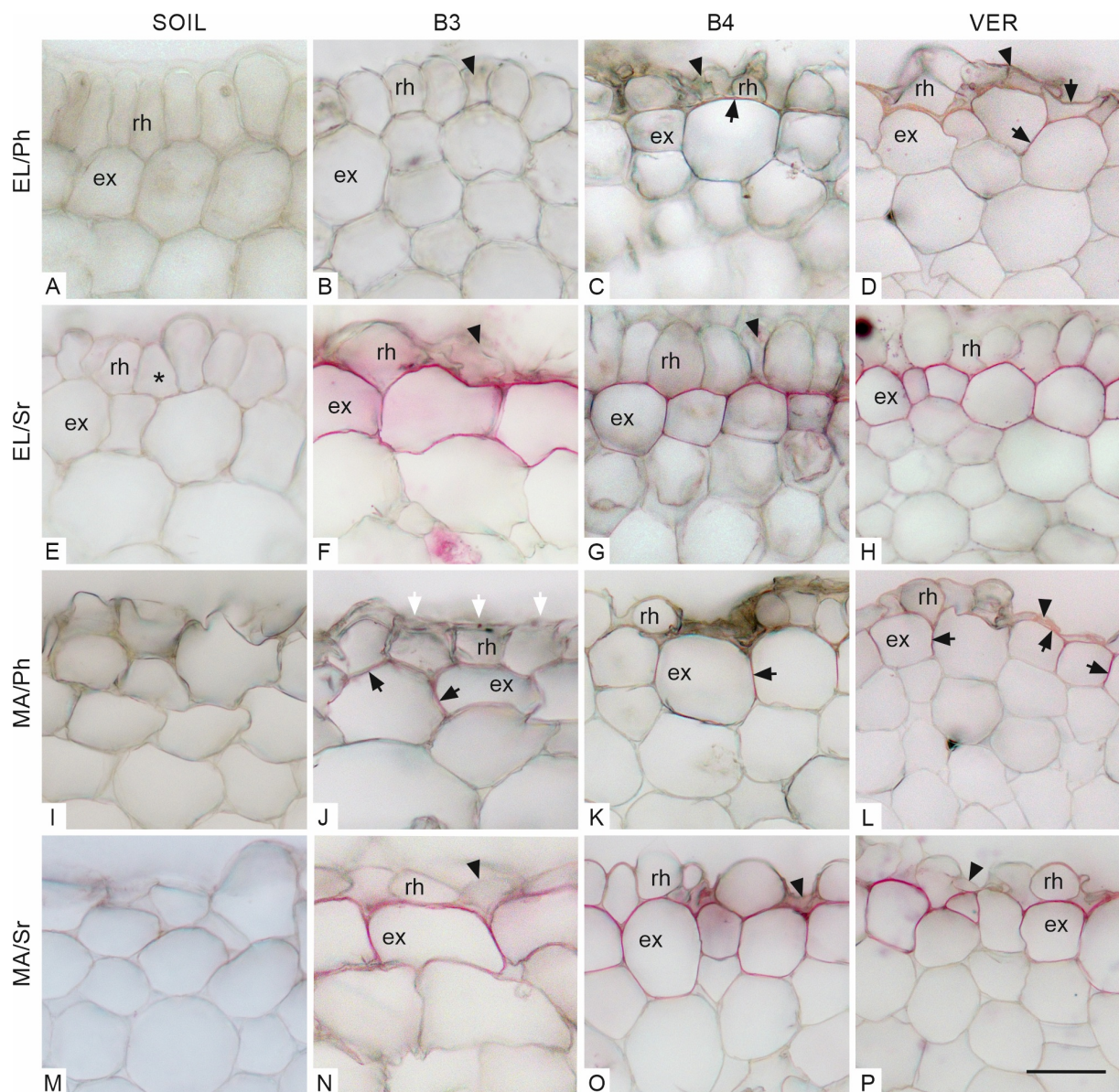


Figure 2 Transverse sections through the outermost maize root tissues in the elongation zone (EL, A–H) and maturation zone (MA, I–P), stained with phloroglucinol (Ph, A–D, I–L) and Sudan red 7B (Sr, E–H, M–P). Arrowheads in B, C, D, F, G, L, N, O, and P indicate damaged or deformed rhizodermal cells. In E, an example of a triangular cell in the rhizodermis is marked with an asterisk. White arrows in J point to local flattening on the root surface at contact with the bead. Lignin detected with phloroglucinol in radial and/or periclinal exodermal cell walls (C, D, J–L) and in rhizodermis (D), indicated by black arrows. Purple staining (Sudan red 7B) in the exodermal cell walls in F–H and N–P indicates the presence of suberin lamellae. Medium: SOIL, B3 beads 3 mm diameter, B4 beads 4 mm diameter, VER vermiculite. Tissue: rh rhizodermis, ex exodermis. Scale bar in P 30 μm (same for all sections in A–P).

late metaxylem. In the roots of the B3, B4, and VER variants, the diameter of the vessels and their distribution varied widely (Figure 4J–L, W–Y), while in the roots of the SOIL variant, the distribution of the vessels was more regular, and the size more uniform (Figure 4I, V). In some vessels, the cell lumen seemed divided into two (Figure 4I–K, X) and sometimes three (Figure 4W) parts.

3.5. Quantitative analyses of the microscopic features

The average cortex thickness in the zone EL ranged from about 189 μm in roots grown in the B4 and VER variants

to 277.3 μm in roots grown in SOIL (Table 3). CT in SOIL roots differed significantly from the values of this parameter in the other variants (Figure 5). In B3 and VER roots, CT in the MA zone was slightly smaller than in the EL zone, while in SOIL and B4 roots, it had increased (Table 3). SOIL roots also showed the highest CT here, while no statistically significant differences between CT values of roots from the B3, B4, and VER variants were detected. Differences between the CT values in zones EL and MA were only found in B4 roots (Figure 5, letters A and B in the left and right plots).

In the elongation zone, the diameter of the vascular cylinder had the lowest value of 204.9 μm in the roots of the VER

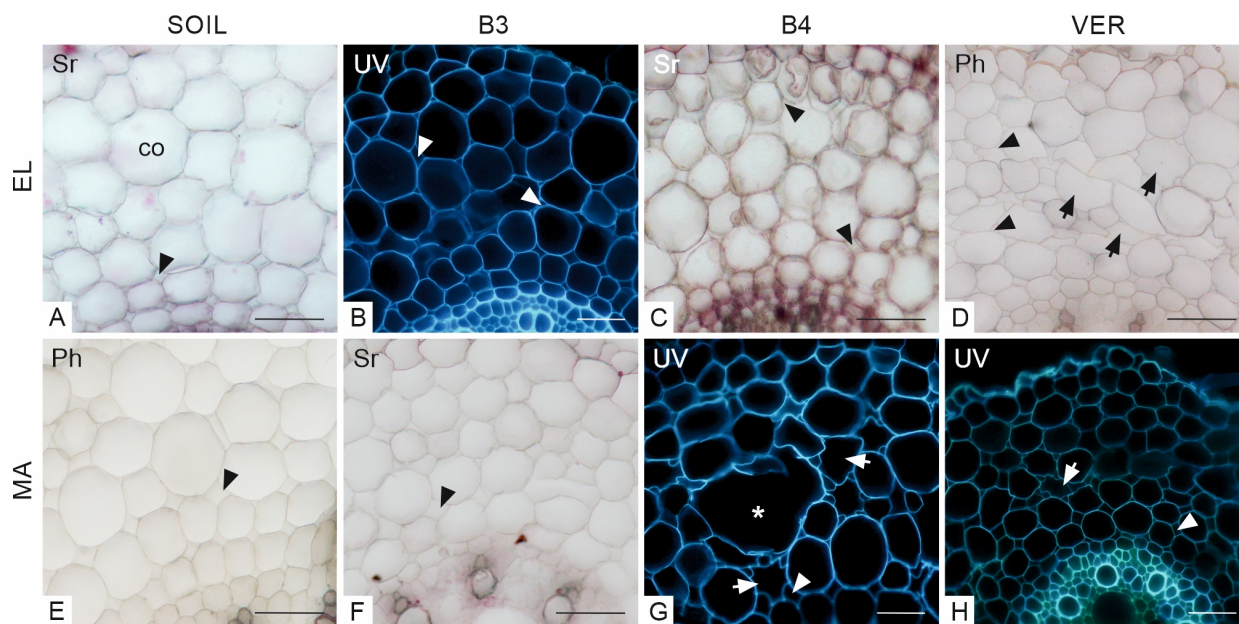


Figure 3 Transverse sections through the maize root cortex in the elongation (EL, A–D) and maturation (MA, E–H) zones. Arrows in D, G, and H indicate deformed cells. An asterisk in G indicates ample air space among cortical cells. The arrowheads point to intercellular spaces. Staining: A, C, F Sudan red 7B (Sr); D, E phloroglucinol (Ph). B, G, H – autofluorescence in UV light. SOIL, B3, B4, VER, same as in Figure 2, co cortex. Scale bars 50 μm.

Table 3 Means ± standard errors of the cortex thickness (CT), the diameter of the vascular cylinder (DVC), and the number of cortical cell layers (NCL) of roots grown in the four experiment variants (SOIL, B3, B4, and VER, same as in Table 2) in elongation (EL) and maturation (MA) zones.

	EL				MA			
	SOIL	B3	B4	VER	SOIL	B3	B4	VER
CT [μm]	277.3 ± 17.6	203.5 ± 20.7	189.1 ± 3.6	189.0 ± 6.0	311.9 ± 8.4	185 ± 23.0	257.7 ± 5.0	183.6 ± 3.8
DVC [μm]	232.4 ± 6.9	264.2 ± 7.4	226.7 ± 10.4	204.9 ± 4.8	275.9 ± 3.8	289.2 ± 9.2	320.7 ± 2.8	212.6 ± 2.5
NCL	6.3 ± 0.2	5.6 ± 0.2	6.5 ± 0.3	6.8 ± 0.3	7.4 ± 0.3	5.3 ± 0.3	7.7 ± 0.3	6.7 ± 0.3

variant and the highest value of 264.2 μm in the roots of the B3 variant (Table 3). No significant differences between the medians of DVC for roots from SOIL, B3, and B4 variants were found, while the differences between the DVC of the B3 and VER variants were significant (Figure 5). In the maturation zone, the value of this parameter increased in all variants. The most remarkable change was observed for the roots of variant B4, where the DVC increased by almost 100 μm (Table 3). As in the EL zone, the median of the VER variant had the lowest value, and it significantly diverged from the other variants, except for the SOIL (Figure 5). Comparison between medians of DVC in the EL and MA zones showed no significant differences, only for the VER variant. In contrast, for the other variants, the DVC medians were significantly different (Figure 5, letters A and B in the left and right plots).

The number of cortical cell layers in the elongation zone varied slightly between roots growing in different variants: the smallest NCL was in roots growing in beads B3 with a mean value of 5.6 layers, and the largest in roots growing in vermiculite with a mean value of 6.8 (Table 3). A comparison of medians showed statistically significant differences between the B3 and VER variants (Figure 5). In the maturation zone,

the average number of layers ranged from 5.3 to 7.7 in roots growing in the B3 and B4 media, respectively. The median of NCL of roots growing in 3 mm diameter beads differed significantly from the medians of the other variants except for the VER variant (Figure 5). A comparison of the medians of NCL between the EL and MA zones indicated no significant difference between the B3 and VER variants (Figure 5, letters A and B in the left and right plots).

3.6. Quantitative analyses of the mechanical properties

Mechanical tests showed that the highest average tensile modulus was that of roots growing in vermiculite, for which the E_T was about twice that of roots from the soil and nearly three times that of roots from glass beads (Table 4). The Young's modulus of the roots of the two bead variants differed significantly from E_T measured in VER roots. The roots of the SOIL and VER variants did not differ significantly in this feature (Figure 6).

Table 4 shows the values of the tensile (E_T) and bending (E_B) modulus of the roots, Young's modulus of the stele (E_S), and cortex (E_C) estimated from Equations (1)–(3). Similar to the

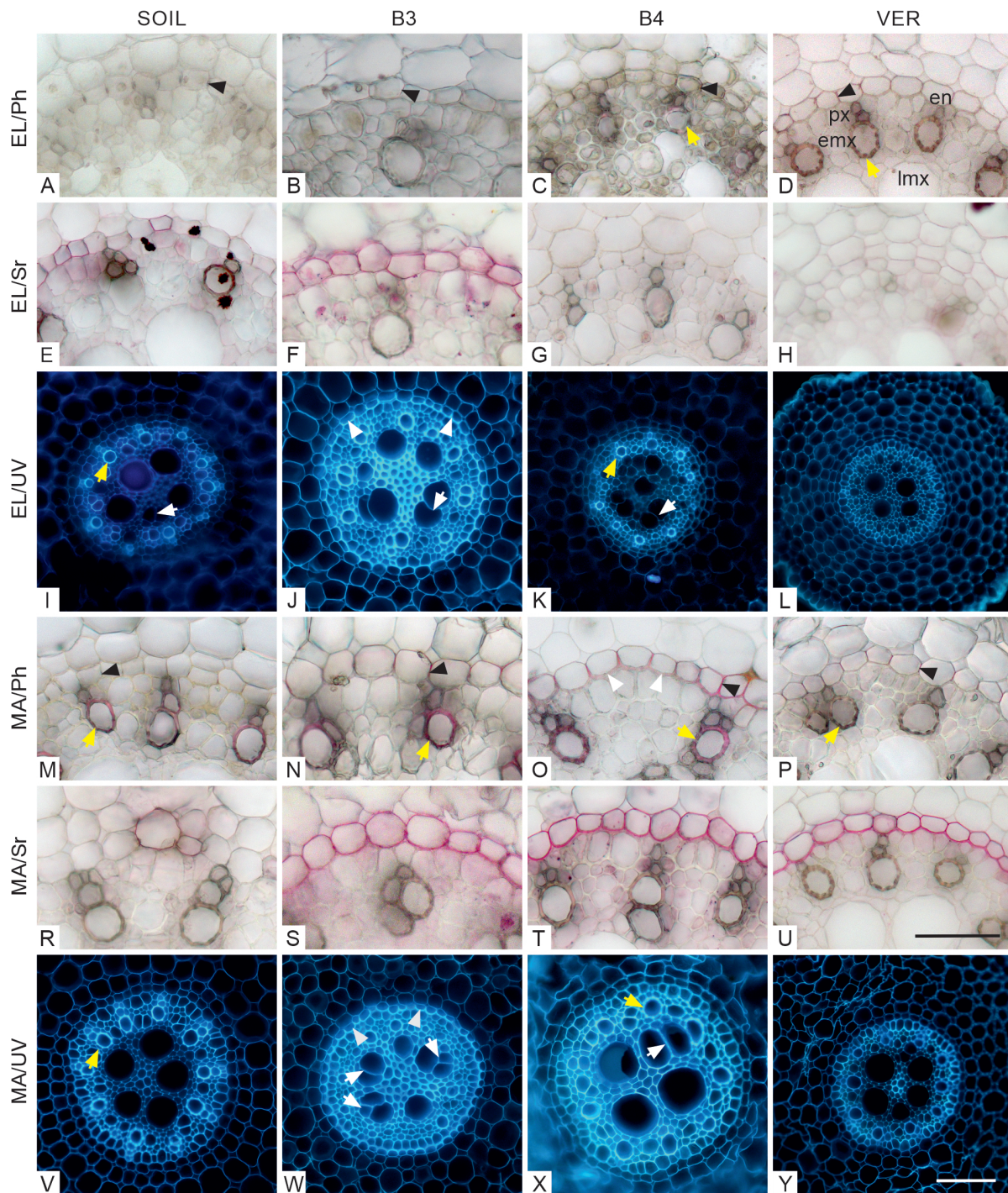


Figure 4 Transverse sections through the vascular cylinder in the elongation (EL, A–L) and maturation (MA, M–Y) zones stained with phloroglucinol (Ph, A–D, M–P) and Sudan red 7B (Sr, E–H, R–U), and visualized in UV light (I–L, V–Y). Black arrowheads in A–D, M–P point to Casparian bands in radial walls of endodermal cells. Tertiary cell wall thickenings of endodermal cells in J, O, and W are indicated by white arrowheads. Endodermal suberin lamellae stained purple in E–F and R–U. White arrows in I–K, and W–X show atypically joined late metaxylem elements. Lignified early metaxylem and protoxylem cells found in roots from all variants are pointed with yellow arrows. Medium: SOIL, B3, B4, VER, same as in Figure 2. Tissue: en endodermis, lmx late metaxylem, emx early metaxylem, px protoxylem. Scale bars in U (referring to sections in A–H, M–U) and Y (referring to UV images in I–L, V–Y) 100 μm .

measured E_T , the model-estimated E_B , E_S , and E_C were the largest for the VER variant roots. However, the most striking were the differences between the small values of E_C and large E_S , indicating that the stele tissues had considerable resistance to mechanical forces. Depending on the experimental variant,

E_S was about seventeen (variant B3), thirty (B4), forty (VER), and ninety (SOIL) times larger than E_C . It should also be noted that while the Young's modulus of the cortex of roots growing in soil was relatively small and comparable to the E_C of roots from variants B3 and B4, the Young's modulus of the stele of

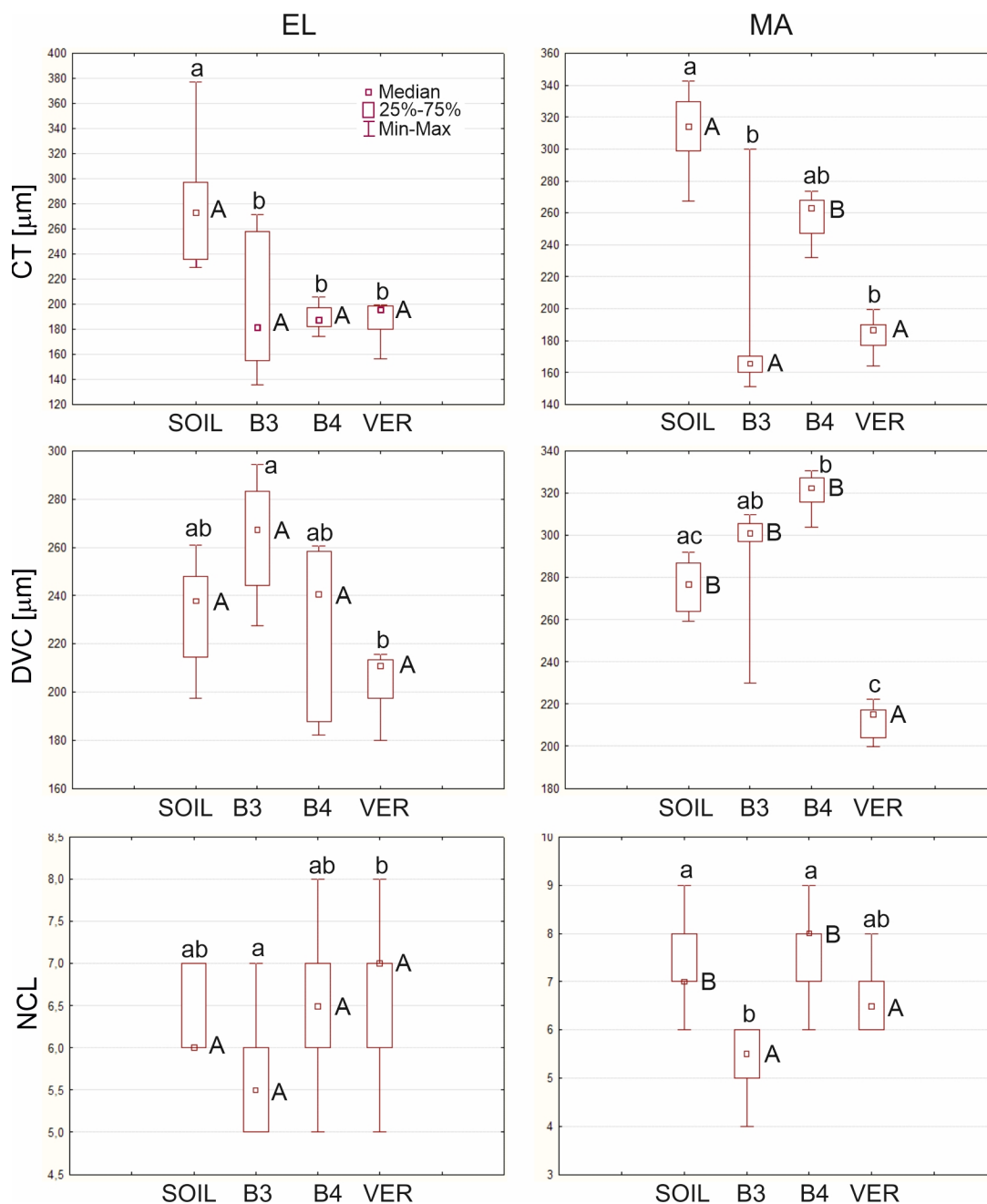


Figure 5 The cortex thickness (CT), the diameter of the vascular cylinder (DVC), and the number of cortical cell layers (NCL) in elongation (EL) and maturation (MA) zones of *Zea* roots grown in four experiment variants (SOIL, B3, B4, and VER, same as in Figure 1). Box and whiskers plots represent medians (small squares), quartiles 1 and 3 (box), and the range of data (whiskers). The same small letters (a, b, c) above the plots indicate statistically insignificant differences between the medians (comparison between variants in the same zone using Kruskal–Wallis nonparametric ANOVA and *post hoc* test of multiple comparisons, $p < 0.05$). The same capital letters (A, B) next to the medians indicate statistically insignificant differences between the medians (comparison between left and right plots concerning two zones for the same variant using U Mann–Whitney test, $p < 0.05$).

roots from the SOIL variant was large, similar to the E_S of roots from vermiculite (Table 4).

4. Discussion

For a growing root, the important characteristics of the medium are density and the size of its particles compared to the radial size of the root apex (Kolb et al., 2017). The media used in our study differed in these characteristics. The

experiment results showed how the physical conditions of the substrate might modify maize root anatomy and mechanical properties.

4.1. The investigated root zones

The experiment considered two root zones: the elongation EL and the maturation MA zone. The EL zone, immediately adjacent to the root apical meristem, is where the cells still

Table 4 Means ± standard errors of Young’s modulus (E_T) measured in the mechanical tests and the estimated (using the mathematical model) values of the bending modulus of the whole samples (E_B), Young’s modulus of the stele (E_S) and cortex (E_C) for the roots grown in the four experiment variants (SOIL, B3, B4, and VER, same as in Table 2).

	SOIL	B3	B4	VER
E_T [MPa]	22.7 ± 20.98	11.7 ± 6.32	13.6 ± 4.92	37.9 ± 10.74
E_B [MPa]	4.26	4.49	4.01	10.20
E_S [MPa]	218.20	49.00	79.00	244.10
E_C [MPa]	2.40	2.80	2.40	5.90

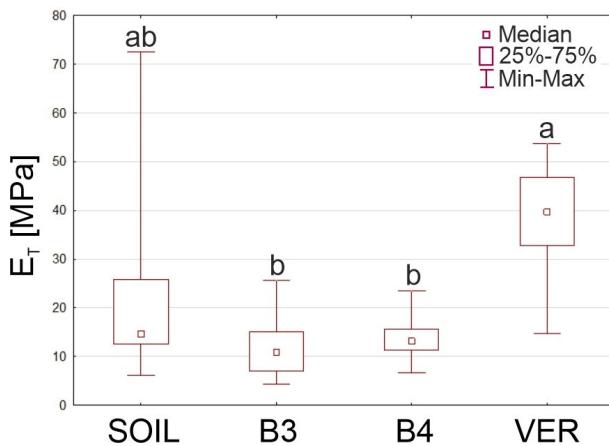


Figure 6 The Young’s modulus (E_T) of *Zea* roots grown in four experiment variants (SOIL, B3, B4, and VER, same as in Figure 1). Box and whiskers plots represent medians (small squares), quartiles 1 and 3 (box), and the range of data (whiskers). The same small letters (a, b, c) above the plots indicate statistically insignificant differences between the medians (based on the Kruskal–Wallis ANOVA and *post hoc* test of multiple comparisons, $p < 0.05$).

grow, so they have yet to reach their final sizes and have not entirely differentiated. In this zone, the growing cells move up along the root axis. In contrast, the MA zone is where the cells have already reached their final sizes and are differentiated, and their positions do not change to the medium because the mature part of the root is anchored in the stratum (Bengough et al., 1997). However, the cells in the MA zone were previously in the EL zone and also underwent movement relative to the medium. Thus, it can be expected that the morphological changes in EL would be minor than in MA since the cells in the MA zone have traveled a much longer distance to their current position, being longer exposed to friction against medium particles, while those in the EL zone are at the beginning of this path. Below, the effect of the medium on the root cell arrangement and the root form in the two distinguished zones is analyzed.

4.2. Anatomical and morphological alterations in the EL and MA zones. Rhizodermis and cortex

The shape of the root was altered by media composed of beads that caused flattening on the root surface (Figure 2). A similar effect was observed in the roots of cereal crops grown in compacted soil in which surface flattening and invaginations

were transferred into deformations in the cell arrangement of the peripheral and deeper-lying cell layers (Lipiec et al., 2012). Growth media had different effects on the integrity of the rhizodermis. In the roots from beads, rhizodermal cells were malformed, and in the VER roots, they were the most damaged (Figure 2). This may be related to the fact that the vermiculite particles have a lamellar structure that can injure the rhizodermis. However, rhizodermis death may also result from degradation by microorganisms under field conditions or even occur in near-optimal laboratory conditions (Enstone et al., 2002). The effect of the medium on the outermost layer of root cells is poorly described in the literature. An example to compare our results to is the research of Lipiec and colleagues (2012), who showed seriously damaged epidermis in roots grown in compacted soil, eventually leading to penetration of these cells by soil particles.

The growth media also affected the root cortex. In the roots of all variants, except SOIL, the cell pattern was significantly disturbed (Figure 3). The roots differed in terms of morphometric features (Figure 5, Table 3). In general, in a lightweight, low-density medium (vermiculite), the radial dimension of the cortex was small. In contrast, it was significantly larger in a high-density medium (soil and glass beads). The conclusion is in line with the results of previous studies in which roots grown in media with increased density or in media subjected to external mechanical pressure showed increased cortex thickness (Hanbury & Atwell, 2005; Vanhees et al., 2022; Veen, 1982).

In the cortex of some roots of the B4 variant, in the MA zone, large intercellular spaces were present (Figure 3G), which might indicate aerenchyma formation. In maize roots, this tissue is formed in response to various environmental stresses, like hypoxia, mechanical factors, or nutrient starvation (Bouranis et al., 2003; He et al., 1996) to reduce the root respiration costs in conditions of limited oxygen availability (Vanhees et al., 2020). The environment of glass beads, whose diameters are larger and pores are smaller than the diameter of the root apex, certainly generates mechanical stress for the growing root, which has to push through narrow gaps. Moreover, because of the small size of the pores, water can be retained in them, causing hypoxia. Considering the conditions of mechanical stress, we see that it is easiest for the root to push through vermiculite, a light-medium with movable particles. At the same time, it is hardest through glass beads, even though their density is lower than that of soil. However, unlike soil particles, the beads are difficult to move. As a result, a growing root can only move through the pores between the beads. This condition makes the glass beads the most challenging environment in terms of mechanical

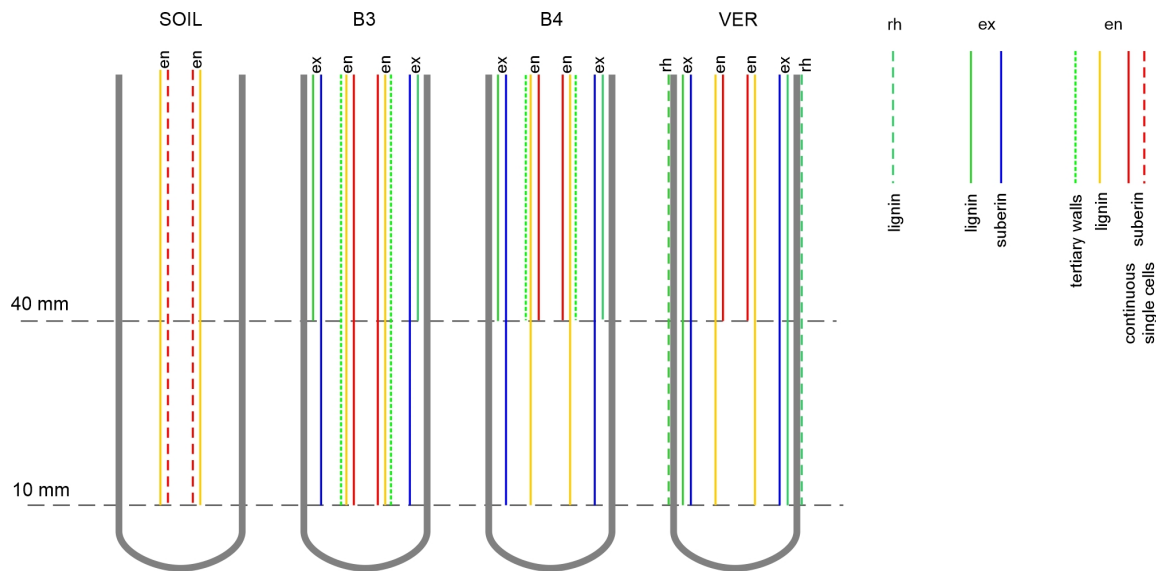


Figure 7 Diagram of exodermis and endodermis development in maize roots grown in conditions of the four experimental variants. Horizontal dashed lines indicate cross-sectional levels corresponding to the EL (10 mm) and MA (40 mm) zones. In exodermis and endodermis, lignin refers to Casparian bands in radial walls, and suberin refers to suberin lamella formation. The experiment variants SOIL, B3, B4, and VER, the same as in Figure 2. Tissue: rh rhizodermis, ex exodermis, en endodermis.

stress. However, it is difficult to say why the intercellular spaces appeared in our experiment only in the roots of the B4 variant and not of the B3 variant since both the pore sizes and densities of the two media were similar. In roots of grass subjected to water stress, the occurrence of large intercellular spaces within the cortex is accompanied by the formation of multi-layered rings of thick-walled, densely packed small cells in the outer cortex, which is interpreted as a mechanical strengthening of the root structure with high porosity (Striker et al., 2007). In our experiment, we did not observe such a marked ring of cells. However, in the roots of some variants, the earlier deposition of hydrophobic substances, lignin, and suberin, in the outermost layer of the cortex (exodermis) and in the rhizodermis was observed, which will be discussed in the next section.

4.3. Deposition of hydrophobic substances in the cell walls. Formation of exodermis and endodermis

Both exodermis and endodermis had undergone developmental changes, schematically illustrated in Figure 7. In roots from beads and vermiculite, exodermis reached developmental stage II already in the EL zone. In roots from the soil, suberin lamella was not detected in either the EL or MA zones (Figure 2). Endodermis development was also accelerated in the roots grown in beads and in vermiculite compared to the roots grown in soil. The earliest differentiation of the endodermis was observed in the roots of the B3 variant, in which, at the level of the upper border of the elongation zone (10 mm from the root tip), the U-shaped tertiary walls appeared (Figure 4). The accelerated differentiation of both tissues is usually a root response to various stresses (Enstone et al., 2002), including mechanical stress (Wilson & Robards, 1978). Also, the formation of the tertiary walls in the endodermis is considered a part of the reinforcement of the mechanical structure of the root (Enstone et al., 2002).

In the EL zone of roots from glass beads, Casparian bands, typical of stage I of the tissue development, were not present in exodermis even though the suberin lamellae, proving stage II, was detected. It is possible that the Casparian bands were not detectable by the staining method or that suberin deposition preceded the formation of the bands in time. The former explanation seems unlikely since the Casparian bands were detected by the same method in the MA zone of these roots and in the roots of the variant VER. On the other hand, the second explanation seems plausible, since a similar presence of suberin lamellae in the absence of Casparian bands was reported by Tylová et al. (2017) in primary maize roots grown under oxygen deficiency stress in hydroponic conditions.

In roots of all variants except SOIL, the outer periclinal walls of exodermis were incrustated with lignin, and in the VER roots, lignin was also detected in rhizodermis (Figure 2). Lignin improves the stability of the root cell walls thus affecting the mechanical strengthening of the root structure (Degenhardt & Gimmler, 2000). While the need to strengthen the structure in roots growing in glass beads is clear, a modification of this kind in roots growing in light vermiculite may be puzzling unless we consider that not only the density but also the shape and arrangement of the medium particles may affect the morphology and growth of the root. On the other hand, the roots of the VER variant had the smallest diameters and were flaccid, although difficult to break, so they could be compared to string, which is irresistible to bending but resistant to stretching. Thus, in the first case (beads), the stimulus for lignin deposition in the exodermis was the resistance of a highly packed medium, while in the second case (vermiculite), it was the flaccid structure of the root caused by the lack of resistance from the light medium. Can we then assume that the root uses the same strategy (lignification) to respond to opposite types of stimuli? Answering this question requires independent research.

4.4. Anatomical and morphological alterations in the EL and MA zones. Vascular cylinder

In all roots, the diameter of the vascular cylinder (DVC) was larger in the MA zone than in the EL zone (Figure 5). It was the smallest in roots growing in vermiculite (lowest density), standing apart from the values of DVC in roots from the other variants (Table 3, Figure 5). This shows that the medium density, directly related to the presence of mechanical stress exerted on the root, may be a factor affecting DVC. Other reports show that DVC may either increase or decrease in the presence of mechanical stress, depending on the plant species (Bengough et al., 1997; Lipiec et al., 2012). Also, the area (Lipiec et al., 2012) and shape of the vascular cylinder may change, as in some roots from the SOIL variant of our experiment (Figure 4). Another response to the experimental conditions within the vascular cylinder was the disrupted arrangement of the metaxylem elements and visible differences in their sizes, especially in the variants using the bead substrate (Figure 4). Thus the growth medium may also affect the cell pattern of the innermost tissues.

Eventually, it is worth mentioning the atypical junction of two or three adjacent late metaxylem vessels observed in numerous cross-sections through the roots (Figure 4). Since this occurred in the roots of all variants, it is difficult to specify how the media might have affected the formation of such junctions. Barlow and Adam (1989), who observed similar anatomical changes in maize roots exposed to low temperatures, suggested that this effect might be due to the particular sensitivity of the vessels to stress conditions. As shown by Hejnowicz (2005), such forms can occur on cross sections where the end portions of neighboring tracheal elements are adjacent to each other. They can also be an image of more complex structures, such as branching vessels.

4.5. Differences in macroscopic morphological and mechanical properties of roots

Young's modulus refers to the material's tensile stiffness, which means that roots with high E_T are more resistant to buckling. Here, the thinnest roots of the VER variant (Table 2, Table S1), whose vascular cylinder had the smallest diameter (Table 3), proved to be the most resistant to buckling. This confirms some previous observations that the tensile strength of roots is higher the smaller the root diameter and vascular cylinder diameter (Chimungu et al., 2015; Loades et al., 2015). In addition, roots growing in vermiculite were the longest (Table 2); in other words, they grew the fastest, suggesting that large E_T was associated with a higher root elongation rate. Interestingly, the bending modulus (E_B), which was estimated from the model (Onoda et al., 2015), had a comparable and quite small value for the roots of the high-density media, while for the roots growing in light vermiculite, E_B was more than double that of the roots of the other variants (Table 4). Roots growing in rigid glass beads are forced to search for free spaces between the particles of the medium, so they undergo bending anyway. For these roots, small E_B is therefore advantageous. The soil that compresses and supports the root prevents it from bending; it seems then that the roots grown in this medium do not need large E_B , however, this implication requires extra research. In vermiculite, on the other hand, there are a lot of free spaces between the aggregates, so the

root needs to have a larger E_B to keep itself from bending. It is also worth noting the E_B/E_T ratio. For the roots of the beads variants, it is about 1/3, while for the vermiculite roots, this ratio is less than 1/4, and for soil roots, it is about 1/5, that is, E_T here is about five times greater than E_B . Given the overall good condition of the soil roots, can we assume that such a distribution of mechanical properties is favorable for the growing root? Again, more study is needed to answer this question.

Using a mechanical model (Onoda et al., 2015) enabled estimating Young's modulus for stele and cortex. However, there is no data to compare them with because they cannot be determined experimentally in a living root, and model descriptions are lacking. Anyway, according to the estimates presented, E_S exceeds E_C many times (Table 4). This result is in accordance with the experiment: in tensile tests of maize roots, the cortex underwent failure before the whole root (Chimungu et al., 2015), indicating that the cortex is less resistant to tensile forces. As with E_B , E_C values are comparable for roots of high-density media, while vermiculite roots show about twice as much E_C . The Young's modulus of the stele was many times larger than the E_C of the root of all variants, which shows that E_S contributes significantly to the total E_T of the root (see also Chimungu et al., 2015). E_S was highest in vermiculite and soil roots, which were media with extreme physical characteristics. The large E_C and E_S of the VER variant roots may indicate the need to strengthen their tissues in a light-medium that does not provide mechanical support.

The question arises about the origin of the high values of the mechanical moduli of vermiculite-cultured roots. The reason can be traced to the anatomical characteristics of these roots. Namely, as described above, in roots growing in light vermiculite and in heavy, rigid glass beads, the maturation of exodermis and endodermis had been accelerated. This process was associated with the mechanical strengthening of the tissues and, consequently, of the entire root, which ultimately resulted in increased tensile strength.

5. Conclusions

The results indicate that the physical conditions of the substrate affect the anatomical traits and mechanical properties of maize roots. The most prominent and deepest-reaching deformations of the cell arrangement occurred in roots growing in vermiculite. However, significant changes were also observed in roots growing in glass beads. In these variants, the cell arrangement of the cortex and vascular cylinder was impaired in addition to early damage of the rhizodermis. Major modifications of the cell arrangement were observed in the root maturation zone than in the elongation zone. The exodermis and endodermis matured earlier in roots grown in beads and vermiculite than in roots grown in soil. The vermiculite roots, which had the smallest cortex thickness and vascular cylinder diameter, were also the most outliers regarding measurable parameters and mechanical properties. Eventually, the soil did not cause severe changes in the cell pattern of the root. Also, the mechanical properties of roots growing in soil (low E_B , high E_T) seem favorable for the organ's growth. Thus, from the point of view of anatomy, a medium with higher density and fine, easily movable particles is more convenient for maize root growth than a medium with low density and light particles or a medium with high density and large unmovable

particles. This paper also offers, for the first time, the method of estimation values of Young's modulus for cortex and stele. The vascular tissues' tensile stiffness exceeds the cortex's tensile stiffness many times over.

6. Supplementary material

The following supplementary material is available for this article:

Table S1. Means \pm standard errors of the length and diameter of the root apical portions used in the tensile test, SOIL, B3, B4, and VER – four experiment variants, same as in Table 2, n – sample size.

References

- Alarcón, M. V., Lloret, P. G., & Salguero, J. (2014). The development of the maize root system: Role of auxin and ethylene. In A. Morte & A. Varma (Eds.), *Root engineering: Basic and applied concepts* (pp. 75–103). Springer. https://doi.org/10.1007/978-3-642-54276-3_5
- Alexander, K. G., & Miller, M. H. (1991). The effect of soil aggregate size on early growth and shoot-root ratio of maize (*Zea mays* L.). *Plant and Soil*, *138*, 189–194. <https://doi.org/10.1007/BF00012245>
- Barlow, P. W., & Adam, J. S. (1989). Anatomical disturbances in primary roots of *Zea mays* following periods of cool temperature. *Environmental and Experimental Botany*, *29*(3), 323–336. [https://doi.org/10.1016/0098-8472\(89\)90006-3](https://doi.org/10.1016/0098-8472(89)90006-3)
- Bengough, A. G., Croser, C., & Pritchard, J. (1997). A biophysical analysis of root growth under mechanical stress. *Plant and Soil*, *189*, 155–164. <https://doi.org/10.1023/A:1004240706284>
- Bouranis, D. L., Chorianopoulou, S. N., Siyiannis, V. F., Protonotarios, V. E., & Hawkesford, M. J. (2003). Aerenchyma formation in roots of maize during sulphate starvation. *Planta*, *217*, 382–391. <https://doi.org/10.1007/s00425-003-1007-6>
- Chalk, P., Gooding, N., Hutten, S., You, Z., & Bedrikovetsky, P. (2012). Pore size distribution from challenge coreflood testing by colloidal flow. *Chemical Engineering Research and Design*, *90*(1), 63–77. <https://doi.org/10.1016/j.cherd.2011.08.018>
- Chimungu, J. G., Loades, K. W., & Lynch, J. P. (2015). Root anatomical phenes predict root penetration ability and biomechanical properties in maize (*Zea mays*). *Journal of Experimental Botany*, *66*(11), 3151–3162. <https://doi.org/10.1093/jxb/erv121>
- Clark, L. J., Price, A. H., Steele, K. A., & Whalley, W. R. (2008). Evidence from near-isogenic lines that root penetration increases with root diameter and bending stiffness in rice. *Functional Plant Biology*, *35*(11), 1163–1171. <https://doi.org/10.1071/FP08132>
- Degenhardt, B., & Gimmler, H. (2000). Cell wall adaptations to multiple environmental stresses in maize roots. *Journal of Experimental Botany*, *51*(344), 595–603. <https://doi.org/10.1093/jexbot/51.344.595>
- Enstone, D. E., Peterson, C. A., & Ma, F. (2002). Root endodermis and exodermis: Structure, function, and responses to the environment. *Journal of Plant Growth Regulation*, *21*, 335–351. <https://doi.org/10.1007/s00344-003-0002-2>
- Gibson, L. J. (2012). The hierarchical structure and mechanics of plant materials. *Journal of the Royal Society Interface*, *9*(76), 2749–2766. <https://doi.org/10.1098/rsif.2012.0341>
- Goodno, B. J., & Gere, J. M. (2020). *Mechanics of materials*. Cengage Learning.
- Goss, M. J., & Drew, M. C. (1972). Effect of mechanical impedance on growth of seedlings. *Agricultural Research Council Letcombe Laboratory Annual Report, 1971*, 35–42.
- Groleau-Renaud, V., Plantureux, S., & Guckert, A. (1998). Influence of plant morphology on root exudation of maize subjected to mechanical impedance in hydroponic conditions. *Plant and Soil*, *201*, 231–239. <https://doi.org/10.1023/A:1004316416034>
- Grzesiak, M. T. (2009). Impact of soil compaction on root architecture, leaf water status, gas exchange and growth of maize and triticale seedlings. *Plant Root*, *3*, 10–16. <https://doi.org/10.3117/plantroot.3.10>
- Hanbury, C. D., & Atwell, B. J. (2005). Growth dynamics of mechanically impeded lupin roots: Does altered morphology induce hypoxia? *Annals of Botany*, *96*(5), 913–924. <https://doi.org/10.1093/aob/mci243>
- Hattori, T., Inanaga, S., Tanimoto, E., Lux, A., Luxová, M., & Sugimoto, Y. (2003). Silicon-induced changes in viscoelastic properties of sorghum root cell walls. *Plant and Cell Physiology*, *44*(7), 743–749. <https://doi.org/10.1093/pcp/pcg090>
- He, C. J., Finlayson, S. A., Drew, M. C., Jordan, W. R., & Morgan, P. W. (1996). Ethylene biosynthesis during aerenchyma formation in roots of maize subjected to mechanical impedance and hypoxia. *Plant Physiology*, *112*(4), 1679–1685. <https://doi.org/10.1104/pp.112.4.1679>
- Hejnowicz, Z. (2005). Unusual metaxylem tracheids in petioles of *Amorphophallus* (Araceae) giant leaves. *Annals of Botany*, *96*(3), 407–412. <https://doi.org/10.1093/aob/mci198>
- Iijima, M., Kato, J., & Taniguchi, A. (2007). Combined soil physical stress of soil drying, anaerobiosis and mechanical impedance to seedling root growth of four crop species. *Plant Production Science*, *10*(4), 451–459. <https://doi.org/10.1626/pps.10.451>
- Karahara, I., Ikeda, A., Kondo, T., & Uetake, Y. (2004). Development of the Casparian strip in primary roots of maize under salt stress. *Planta*, *219*, 41–47. <https://doi.org/10.1007/s00425-004-1208-7>
- Kolb, E., Legué, V., & Bogeat-Triboulot, M. B. (2017). Physical root–soil interactions. *Physical Biology*, *14*(6), Article 065004. <https://doi.org/10.1088/1478-3975/aa90dd>
- Konôpka, B., Pagès, L., & Doussan, C. (2008). Impact of soil compaction heterogeneity and moisture on maize (*Zea mays* L.) root and shoot development. *Plant, Soil and Environment*, *54*(12), 509–519. <https://doi.org/10.17221/429-PSE>
- Lipiec, J., Horn, R., Pietrusiewicz, J., & Siczek, A. (2012). Effects of soil compaction on root elongation and anatomy of different cereal plant species. *Soil and Tillage Research*, *121*, 74–81. <https://doi.org/10.1016/j.still.2012.01.013>
- Loades, K. W., Bengough, A. G., Bransby, M. F., & Hallett, P. D. (2015). Effect of root age on the biomechanics of seminal and nodal roots of barley (*Hordeum vulgare* L.) in

- contrasting soil environments. *Plant and Soil*, 395, 253–261. <https://doi.org/10.1007/s11104-015-2560-z>
- Lux, A., Luxová, M., Abe, J., & Morita, S. (2004). Root cortex: Structural and functional variability and responses to environmental stress. *Root Research*, 13(3), 117–131. <https://doi.org/10.3117/rootres.13.117>
- Onoda, Y., Schieving, F., & Anten, N. P. (2015). A novel method of measuring leaf epidermis and mesophyll stiffness shows the ubiquitous nature of the sandwich structure of leaf laminae in broad-leaved angiosperm species. *Journal of Experimental Botany*, 66(9), 2487–2499. <https://doi.org/10.1093/jxb/erv024>
- Perumalla, C. J., & Peterson, C. A. (1986). Deposition of Casparian bands and suberin lamellae in the exodermis and endodermis of young corn and onion roots. *Canadian Journal of Botany*, 64(9), 1873–1878. <https://doi.org/10.1139/b86-248>
- Peterson, C. A. (1988). Exodermal Casparian bands: Their significance for ion uptake by roots. *Physiologia Plantarum*, 72(1), 204–208. <https://doi.org/10.1111/j.1399-3054.1988.tb06644.x>
- Potocka, I., & Szymanowska-Pułka, J. (2018). Morphological responses of plant roots to mechanical stress. *Annals of Botany*, 122(5), 711–723. <https://doi.org/10.1093/aob/mcy010>
- Potocka, I., Szymanowska-Pułka, J., Karczewski, J., & Nakielski, J. (2011). Effect of mechanical stress on *Zea* root apex. I. Mechanical stress leads to the switch from closed to open meristem organization. *Journal of Experimental Botany*, 62(13), 4583–4593. <https://doi.org/10.1093/jxb/err169>
- Schreiber, L., Hartmann, K., Skrabs, M., & Zeier, J. (1999). Apoplastic barriers in roots: Chemical composition of endodermal and hypodermal cell walls. *Journal of Experimental Botany*, 50(337), 1267–1280. <https://doi.org/10.1093/jxb/50.337.1267>
- Striker, G. G., Insausti, P., Grimoldi, A. A., & Vega, A. S. (2007). Trade-off between root porosity and mechanical strength in species with different types of aerenchyma. *Plant, Cell & Environment*, 30(5), 580–589. <https://doi.org/10.1111/j.1365-3040.2007.01639.x>
- Szymanowska-Pułka, J. (2013). Form matters: Morphological aspects of lateral root development. *Annals of Botany*, 112(9), 1643–1654. <https://doi.org/10.1093/aob/mct231>
- Tanimoto, E., Fujii, S., Yamamoto, R., & Inanaga, S. (2000). Measurement of viscoelastic properties of root cell walls affected by low pH in lateral roots of *Pisum sativum* L. *Plant and Soil*, 226, 21–28. <https://doi.org/10.1023/A:1026460308158>
- Tylová, E., Pecková, E., Blascheová, Z., & Soukup, A. (2017). Casparian bands and suberin lamellae in exodermis of lateral roots: An important trait of roots system response to abiotic stress factors. *Annals of Botany*, 120(1), 71–85. <https://doi.org/10.1093/aob/mcx047>
- Vanhees, D. J., Loades, K. W., Bengough, A. G., Mooney, S. J., & Lynch, J. P. (2020). Root anatomical traits contribute to deeper rooting of maize under compacted field conditions. *Journal of Experimental Botany*, 71(14), 4243–4257. <https://doi.org/10.1093/jxb/eraa165>
- Vanhees, D. J., Schneider, H. M., Sidhu, J. S., Loades, K. W., Bengough, A. G., Bennett, M. J., Pandey, B. K., Brown, K. M., Mooney, S. J., & Lynch, J. P. (2022). Soil penetration by maize roots is negatively related to ethylene-induced thickening. *Plant, Cell & Environment*, 45(3), 789–804. <https://doi.org/10.1111/pce.14175>
- Veen, B. W. (1982). The influence of mechanical impedance on the growth of maize roots. *Plant and Soil*, 66, 101–109. <https://doi.org/10.1007/BF02203407>
- Wilson, A. J., & Robards, A. W. (1978). The ultrastructural development of mechanically impeded barley roots. Effects on the endodermis and pericycle. *Protoplasma*, 95, 255–265. <https://doi.org/10.1007/BF01294454>
- Wilson, A. J., & Robards, A. W. (1979). Some observations of the effects of mechanical impedance upon the ultrastructure of the root caps of barley. *Protoplasma*, 101, 61–72. <https://doi.org/10.1007/BF01293435>